

## Absolute Band Mapping by Combined Angle-Dependent Very-Low-Energy Electron Diffraction and Photoemission: Application to Cu

V. N. Strocov,<sup>1,2,\*</sup> R. Claessen,<sup>1</sup> G. Nicolay,<sup>1</sup> S. Hüfner,<sup>1</sup> A. Kimura,<sup>3</sup> A. Harasawa,<sup>3</sup> S. Shin,<sup>3</sup> A. Kakizaki,<sup>4</sup>  
P. O. Nilsson,<sup>2</sup> H. I. Starnberg,<sup>2</sup> and P. Blaha<sup>5</sup>

<sup>1</sup>*Fachrichtung Experimentalphysik, Universität des Saarlandes, D-66041 Saarbrücken, Germany*

<sup>2</sup>*Department of Physics, Chalmers University of Technology and Göteborg University, SE-41296 Göteborg, Sweden*

<sup>3</sup>*Institute for Solid State Physics, University of Tokyo, Roppongi, Minato-ku, Tokyo 106-8666, Japan*

<sup>4</sup>*Institute of Materials Structure Science, High Energy Accelerator Research Organization (KEK), Ibaraki 305-0801, Japan*

<sup>5</sup>*Institut für Technische Elektrochemie, Technische Universität Wien, A-1060 Wien, Austria*

(Received 18 August 1998)

We present an experimental method to determine the electronic  $E(\mathbf{k})$  band structure in crystalline solids absolutely, i.e., with complete control of the three-dimensional wave vector  $\mathbf{k}$ . Angle-dependent very-low-energy electron diffraction is first applied to determine the unoccupied states whose  $\mathbf{k}$  is located on a high-symmetry line parallel to the surface. Photoemission via these states, employing the constant-final-state mode, is then utilized to map the valence bands along this line. We demonstrate the method by application to Cu, and find significant deviation from free-electron-like behavior in the unoccupied states, and from density-functional theory in the occupied states. [S0031-9007(98)07792-8]

PACS numbers: 71.20.-b, 79.20.Kz, 79.60.-i

Angle-resolved photoemission (PE) spectroscopy is the principal experimental method for  $E(\mathbf{k})$  band structure determination in crystalline solids [1,2]. The measured photocurrent contains information on the occupied bands through the conservation of energy and surface-parallel momentum  $\mathbf{k}_{\parallel}$  in the PE process. The very existence of a surface, however, breaks the translational invariance normal to it, and therefore the perpendicular component  $k_{\perp}$  is no longer a conserved quantity. Control over the three-dimensional wave vector  $\mathbf{k}$  can be regained, if the  $E(\mathbf{k})$  dispersion of the PE final bands is known. Though often assumed, the free-electron approximation for the final states frequently fails, because these bands are generally far more complicated [3–5]. To circumvent the problem, several schemes for absolute PE band mapping have been developed such as, e.g., triangulation [2,6]. They all are, however, restricted to some particular points in  $\mathbf{k}$  space and in most cases not very practical.

It has recently been demonstrated that the unoccupied upper bands (above the vacuum level  $E_{\text{vac}}$ ) can be directly determined by very-low-energy electron diffraction (VLEED), based on the fact that the PE final states are time-reversed LEED states [7]. The LEED reflectivity  $R$  (or, equivalently, the electron transmission  $T = 1 - R$  from the vacuum into the crystal) will undergo rapid variations whenever for a given  $\mathbf{k}_{\parallel}$  the energy of the incident electrons passes through a critical point (CP) in the corresponding *perpendicular* final-state dispersion  $E(k_{\perp})$  (e.g., the edge of a local band gap), provided that the relevant band couples sufficiently strongly to the vacuum. Thus, the extrema in the differential transmission  $dT/dE$  reveal the location of the CPs [8,9]. The full  $E(k_{\perp})$  dispersion may then be obtained by fitting a semiempirical band calculation to the experimental CPs. This method has re-

cently been applied to layered materials with strongly non-free-electron-like upper bands and utilized successfully for absolute band mapping from normal emission PE [4].

In this Letter, we introduce an alternative method for absolute band mapping, which combines angle-dependent VLEED to determine the CPs on high-symmetry lines of the Brillouin zone (BZ), with constant final state (CFS) PE from the corresponding final-state band gaps [10]. The method does not employ fitting schemes, and is therefore more direct and accurate. It allows the full utilization of off-normal PE spectra and thus absolute band mapping along different high-symmetry lines with only one surface orientation. We demonstrate the usefulness of the method by application to Cu, a material for which the occupied band structure has intensively been studied [11]. It is found that (i) the unoccupied  $E(\mathbf{k})$  dispersions significantly deviate from free-electron-like behavior, and (ii) the measured valence band  $E(\mathbf{k})$  displays strong and consistent deviations from state-of-the-art density-functional band calculations. The details of our work will be presented elsewhere [12].

*Idea.*—The VLEED-CFS PE method determines band dispersions along BZ directions in symmetry planes parallel to the surface. First, one performs angle-dependent VLEED measurements varying the wave vector  $\mathbf{K}_{\parallel}$  of the incident electrons along the chosen BZ direction. The CPs in the symmetry plane (the lower and upper edge of a local band gap) show up as a characteristic minimum-maximum structure in  $dT/dE$  (see Fig. 1). These CPs line up to a pair of unoccupied  $E(\mathbf{k}_{\parallel})$  dispersions in the symmetry plane. Second, with the final-state energy for each  $\mathbf{K}_{\parallel}$  chosen to lie between these bands (i.e., in the band gap) one performs angle-dependent CFS PE measurements.  $\mathbf{k}$  is thus pinned in the symmetry plane, and the peak

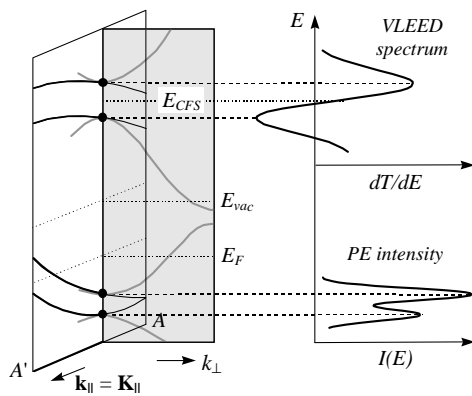


FIG. 1. Schematic illustration of the angle-dependent VLEED-CFS PE method.  $AA'$  is a direction in a symmetry plane parallel to the surface.

positions in the PE spectra directly yield the valence band dispersion along the chosen BZ line.

The method inherently employs photoemission from band gap states, which for the semi-infinite crystal are Bloch waves with complex  $k_{\perp}$ , damped into the crystal by elastic scattering off the crystal potential. However, any qualitative difference between damped and propagating Bloch waves disappears in an interacting excited-state picture [7,9]: all Bloch waves are damped by the electron absorption  $V_i$ , with the overall damping somewhat stronger in the band gaps.

For an application of the method to an fcc metal such as Cu, the (110) surface is most convenient. It gives access to the entire surface-parallel symmetry plane  $\Gamma K L U X$ .

*Unoccupied states by VLEED.*—The VLEED experiment was performed with a standard four-grid LEED unit operated in the retarding field mode [13]. The resulting data, i.e., the extremal points of  $dT/dE$ , yield the  $E(\mathbf{k}_{\parallel})$  map of Fig. 3. The points are gray-shaded proportional to  $-\frac{d^2}{dE^2}(dT/dE)$ , whose sign distinguishes the minima and maxima in  $dT/dE$ , and whose value characterizes the accuracy of their location rather than intensity. The experimental  $E(\mathbf{k}_{\parallel})$  map is basically a direct image of the edges of unoccupied upper bands (except for those which couple too weakly to the vacuum).

For the interpretation of the VLEED data, a general idea of the upper band configuration is helpful, which is achieved by qualitative comparison to an empirical pseudopotential band calculation. As an example, Fig. 2(a) shows the measured normal incidence ( $\mathbf{K}_{\parallel} = 0$ ) VLEED spectrum. Through parallel momentum conservation it probes the  $\Gamma K$  line of the BZ ( $\mathbf{k}_{\parallel} = \mathbf{K}_{\parallel}$ ) and, via surface Umklapp ( $\mathbf{k}_{\parallel} = \mathbf{K}_{\parallel} + 2\bar{\Gamma}\bar{Y}$ ), also  $UX$ . Figure 2(b) shows the corresponding  $E(k_{\perp})$  of the bulk crystal, assuming the no-absorption approximation ( $V_i = 0, k_{\perp}$  real). The gray scale indicates the strength of the vacuum-crystal coupling of the bands, quantified by the partial currents absorbed by the crystal [9,14]. For a semi-infinite crystal and in the presence of excited-state damping mod-

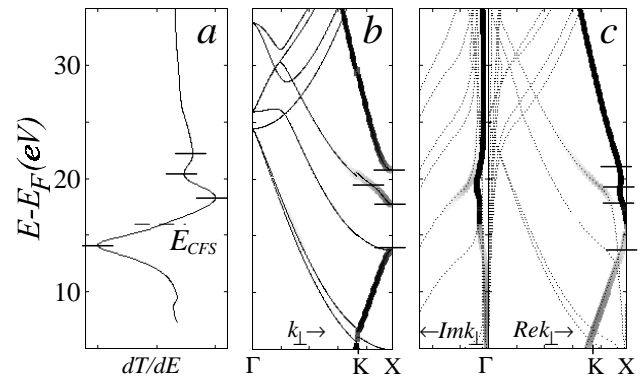


FIG. 2. Differential VLEED spectrum  $dT/dE$  for normal incidence (a); corresponding  $E(k_{\perp})$  reference calculations for a bulk crystal with no absorption,  $V_i = 0$  (b); and a semi-infinite crystal with realistic  $V_i$  (c). The gray scale represents the vacuum-crystal coupling. The horizontal tickmarks indicate the correspondence of the  $dT/dE$  extrema to the CPs of the strongly coupling bands.

eled by a realistic  $V_i \neq 0$  [15] [Fig. 2(c)],  $k_{\perp}$  becomes complex and the  $E(\text{Re } k_{\perp})$  bands smoothen, with the CPs appearing now as inflection points (for details of the calculation, see [9,14]). In any case, the  $dT/dE$  extrema are directly connected to the CPs of the strongly coupling bands and immediately give their energies. In Fig. 2(c),  $E(\text{Re } k_{\perp})$  intersects the surface-parallel  $\Gamma K L U X$  plane (i.e., the  $X$  point) at an energy nearly halfway between the lower two CPs. This position is therefore chosen as the final-state energy  $E_{CFS}$  for the CFS PE measurement.

Proceeding in this manner also for the off-normal VLEED spectra, we have obtained the PE final-state energies pertinent to the  $\Gamma K L U X$  plane for the entire  $\mathbf{k}_{\parallel}$  range of interest, displayed in Fig. 3 as bold dashed

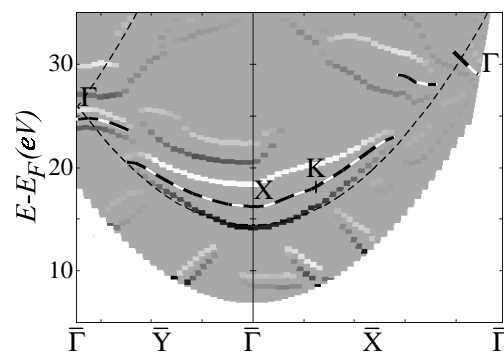


FIG. 3. Experimental upper bands derived from the VLEED  $dT/dE$  extrema. Their shading reflects a logarithmic gray scale proportional to  $-\frac{d^2(dT/dE)}{dE^2}$ , on top of the zero-level gray scale; dark (light) points correspond to  $dT/dE$  minima (maxima). The bold dashed curves show the bands of the final-state energies chosen for the CFS PE experiment, with the high-symmetry points in the  $\Gamma K L U X$  plane indicated; the thin dashed curve is their free-electron approximation. The region below  $E_{\text{vac}} + \frac{\hbar^2 K_{\parallel}^2}{2m} + 2 \text{ eV}$  is clipped.

curves. These energies have discontinuities in regions of extended multiple-band hybridization where the principal coupling band disperses almost vertically [cf. Fig. 2(c)].

*Occupied states by CFS PE.*—The PE measurements were carried out at beam line 18-A of the Photon Factory using an ADES-500 photoelectron spectrometer. The CFS spectra were normalized to the incident photon flux from the PE current of the refocusing mirror.

For an unbiased representation of the PE data, Fig. 4 displays a map of the negative second derivative  $-\frac{d^2I}{dE^2}$  of the photocurrent, cutoff below a threshold to suppress negative values and noise, in the  $(E, \mathbf{k}_{\parallel})$  plane. The peaks in this map have their maxima located at the position of the PE peaks, with the width reflecting the width of the PE peaks and shoulders (the error bars are in fact much smaller). This map is basically a direct image of the occupied valence bands (except for those whose matrix element is too small). The experimental bands are easily identified from the band calculation also shown in Fig. 4.

As a first test of our method we checked the internal consistency of the PE data. Both the measured  $d$  bands as well as the highly dispersive  $sp$  bands show a smooth dispersion, even where the final-state energies undergo discontinuities. As a critical test, we took constant- $\mathbf{k}_{\parallel}$  CFS PE series in such regions, scanning the final-state energy through the discontinuity. Although the intensity varied considerably, the peak binding energies remained stable within  $\pm 50$  meV.

Second, we compared our data with conventional band mapping results along  $\Gamma X$  [16] and  $\Gamma K(U)X$  [17] and found, apart from intensities, excellent correspondence. Note, in particular, that our data, covering almost the entire body of previous work, were obtained in one single experiment. Moreover, for the first time it has become possible to measure the  $sp$  band along the entire  $\Gamma X$ ; its mapping by conventional techniques is troublesome because of the upper band doublet on the (100) surface [9,16].

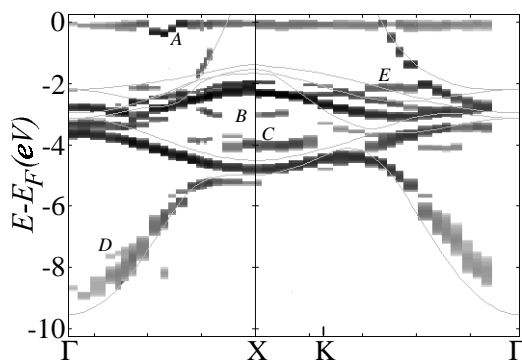


FIG. 4. Experimental valence bands obtained by CFS PE and displayed as a  $-\frac{d^2I}{dE^2}$  logarithmic gray-scale map, on top of the GGA-DFT bands obtained by the FLAPW calculation. The nondispersive structure at  $E_F$  results from the Fermi edge. Note that the energy scale is different from Fig. 3.

Our data contain several structures additional to the expectations from band calculations. Feature *A* (Fig. 4) is a documented surface state [11]; features *B* and *C* near the  $X$  point were reported in [17] and attributed to non- $k_{\perp}$ -conserving transitions. Feature *D* appears in a region of multiple upper band hybridization and is presumably related to excitation to a less strongly coupling band in the BZ interior. Structure *E*, already observed in Ref. [17] using a completely different geometry, seems to be inconsistent with any of the above explanations and will be discussed elsewhere [12].

The results convincingly demonstrate that the combination of VLEED and CFS PE represents a powerful and efficient method for absolute, i.e., truly  $\mathbf{k}$ -resolving band mapping of both the occupied valence band states and the PE final states.

A characteristic feature of our method is photoemission out of final-state band gaps, where the Bloch wave damping  $\text{Im } k_{\perp}$  gets somewhat enhanced (cf. Fig. 2). This might seem a weakness of the method: As  $\text{Im } k_{\perp}$  determines the  $k_{\perp}$  broadening of the PE peak (given by  $\delta k_{\perp} = 2 \text{Im } k_{\perp}$ ) and the transition occurs around an extremal point of the initial state  $E(k_{\perp})$ , the resulting  $k_{\perp}$  averaging combined with the initial state lifetime broadening  $\delta E$  would tend to shift the PE peak towards the band interior. An analysis of the effect based on parameters relevant for our experimental data has shown, however, that the shift remains below 0.1–0.2 eV even in the most critical cases; these numbers do not exceed typical shifts due to nonlinearity of initial bands in conventional band mapping. In practice, our method is more accurate: the enhancement of  $\text{Im } k_{\perp}$  in the band gaps is in general considerably smaller than the enhancement due to  $V_i$ . (Figure 2 is an exceptional case of a very large band gap combined with very small  $V_i$ .) As the method may be applied at relatively low  $h\nu$ , for which the final-state  $V_i$  is small, on the whole,  $\text{Im } k_{\perp}$  remains smaller than in conventional band mapping using higher  $h\nu$ . In return, the wave vector accuracy along the direction of band mapping is determined exclusively by the  $\mathbf{k}_{\parallel}$  resolution and thus limited only instrumentally.

The application of the method to Cu yields two interesting observations. First, the VLEED results show that the upper bands of Cu, contrary to common expectation, show significant non-free-electron behavior in the studied energy range (as already noted in, e.g., [3,9]). This is most clearly seen in the  $E(\mathbf{k}_{\parallel})$  map of Fig. 3: the experimentally determined coupling bands in the  $\Gamma K L U X$  plane (chosen as the CFS energies) deviate dramatically from the corresponding free-electron band [17] and feature large band gaps. One might speculate that the surface-perpendicular dispersion  $E(\text{Re } k_{\perp})$ , through smoothing in the excited state [Fig. 2(c)], remains nevertheless free-electron-like. This picture, however, fails where several bands form an extended hybridization region of an energy width comparable to  $V_i$ . Rather,  $E(\text{Re } k_{\perp})$  goes nearly vertically along the whole region. This behavior

is confirmed by the constant- $k_{\parallel}$  CFS PE series discussed above.

Second, we find significant deviations between the measured valence bands and density-functional theory (DFT). In Fig. 4, we compare our experimental results, which as discussed above are in complete agreement with the previous PE data, to a new state-of-the-art DFT calculation which used the generalized gradient approximation (GGA) for the density-functional [18] and a relativistic self-consistent full-potential linearized augmented plane wave (FLAPW) method [19]. Previous comparisons between PE and band theory [11] were less conclusive, because the theoretical methods were less advanced at the time, as reflected by considerable scatter between the various calculations; now all state-of-the-art calculations produce almost identical results. Although our DFT calculation predicts the overall band configuration correctly, the entire  $d$ -band manifold is experimentally found  $\sim 0.5$  eV lower than calculated. The bottom of the  $sp$  band appears higher than in the theory, with the shift of its bottom, corrected from the intrinsic in-band shifting, being  $\sim 0.5$  eV (the accuracy is limited to  $\pm 0.3$  eV by poor signal/noise ratio and an asymmetric peak shape). The shift in the  $sp$  band is similar to that observed in Na [20]. There are, in principle, two fundamental origins for the observed deviations between PE and DFT results: (i) The true exchange-correlation part of the density functional is not known and therefore any DFT calculation has to resort to a suitable approximation, in our case the GGA; (ii) DFT describes ground state properties (notwithstanding the problem of the physical meaning of DFT eigenvalues), whereas PE probes the single-particle excitations characterized by additional self-energy corrections to the exchange correlation. Although without solid theoretical proof, the second effect is believed to dominate. Existing theoretical estimates of the self-energy corrections in the Cu  $3d$  bands [21], correctly describing the sign, largely underestimated their magnitude ( $\sim 0.1$  eV). While deviations from band theory are known to be large in systems with an open  $3d$  shell (e.g., Ni) due to drastic self-energy effects, it is intriguing to find them still so pronounced in the much less correlated Cu metal.

In conclusion, we have demonstrated that the combination of angle-dependent VLEED and CFS PE provides a powerful tool for accurate and absolute (in the sense of full  $\mathbf{k}$ -space control) band mapping. The main advantage of the method is the natural incorporation of non-free-electron and excited-state effects in the upper bands, which offers an accuracy superior to conventional techniques. A practical aspect is the possibility to obtain a complete band mapping along a variety of BZ directions with a narrow  $h\nu$  range and only one crystal surface. For many crystals having only one stable surface, for example, layered materials, this method is the only way to determine  $E(\mathbf{k})$  in a thorough and well-characterized fashion. Furthermore, as the method allows the use of

rather low photon energies, the best possible  $\mathbf{k}$  resolution can be achieved.

This work was supported by the Deutsche Forschungsgemeinschaft and the Swedish Institute.

---

\*Also with the Institute for High-Performance Computations and Databases, P.O. Box 71, 194291 St. Petersburg, Russia.

- [1] *Angle-Resolved Photoemission*, edited by S.D. Kevan (Elsevier, Amsterdam, 1992).
- [2] S. Hüfner, *Photoelectron Spectroscopy* (Springer-Verlag, Berlin, 1995).
- [3] A. Baalman, M. Neumann, W. Braun, and W. Radlik, *Solid State Commun.* **54**, 583 (1985).
- [4] V.N. Strocov, H. Starnberg, P.O. Nilsson, H.E. Brauer, and L.J. Holleboom, *Phys. Rev. Lett.* **79**, 467 (1997); *J. Phys. Condens. Matter* **10**, 5749 (1998).
- [5] J. Olde, G. Mante, H.-P. Barnscheidt, L. Kipp, J.-C. Kuhr, R. Manzke, M. Skibowski, J. Henk, and W. Schattke, *Phys. Rev. B* **41**, 9958 (1990).
- [6] P.O. Nilsson and N. Dahlback, *Solid State Commun.* **29**, 303 (1979); P. Heinman, M. Miosaga, and H. Neddermeyer, *Solid State Commun.* **29**, 467 (1979).
- [7] P.J. Feibelman and D.E. Eastman, *Phys. Rev. B* **10**, 4932 (1974); J.B. Pendry, *Surf. Sci.* **57**, 679 (1976).
- [8] V.N. Strocov, *Solid State Commun.* **78**, 545 (1991); *Int. J. Mod. Phys. B* **9**, 1755 (1995).
- [9] V.N. Strocov, H. Starnberg, and P.O. Nilsson, *J. Phys. Condens. Matter* **8**, 7539 (1996); *Phys. Rev. B* **56**, 1717 (1997).
- [10] R. Courths, H. Wern, G. Leschik, and S. Hüfner, *Z. Phys. B* **74**, 233 (1989).
- [11] R. Courths and S. Hüfner, *Phys. Rep.* **112**, 53 (1984); R. Matzdorf, *Surf. Sci. Rep.* **30**, 153 (1998).
- [12] V.N. Strocov *et al.* (to be published).
- [13] V.N. Strocov, *Meas. Sci. Technol.* **7**, 1636 (1996).
- [14] V.N. Strocov, *Solid State Commun.* **106**, 101 (1997).
- [15] A. Goldmann, W. Altmann, and V. Dose, *Solid State Commun.* **79**, 511 (1991).
- [16] J.A. Knapp, F.J. Himpsel, and D.E. Eastman, *Phys. Rev. B* **19**, 4952 (1979); S.C. Wu, J. Sokolov, C.K.C. Lok, J. Quinn, Y.S. Li, D. Tian, and F. Jona, *Phys. Rev. B* **39**, 12 891 (1989).
- [17] P. Thiry, Ph.D. thesis, University of Paris, 1979; Y. Petroff and P. Thiry, *Appl. Opt.* **19**, 3957 (1980).
- [18] J.P. Perdew, K. Burke, and M. Ernzerhof, *Phys. Rev. Lett.* **77**, 3865 (1996). The bands obtained by the GGA are almost indistinguishable from those using the local density approximation (LDA).
- [19] P. Blaha, K. Schwarz, and J. Luitz, *WIEN97* (Vienna University of Technology, Vienna, 1997). [Improved version of P. Blaha, K. Schwarz, P. Sorantin, and S.B. Trickey, *Comput. Phys. Commun.* **59**, 339 (1990)].
- [20] E. Jensen and E.W. Plummer, *Phys. Rev. Lett.* **55**, 1912 (1985); H.O. Frota and G.D. Mahan, *Phys. Rev. B* **45**, 6243 (1992).
- [21] P.O. Nilsson and C.G. Larsson, *Phys. Rev. B* **27**, 6143 (1983).